Published in final edited form as:
Arterioscler Thromb Vasc Biol. 2010 August ; 30(8): 1621–1627. doi:10.1161/ATVBAHA.110.208348.

Anti-Thrombogenic Modification of Small-Diameter Microfibrous Vascular Grafts

Craig K. Hashi, Ph.D.[1,2], **Nikita Derugin, M.A.**[3], **Randall Raphael R. Janairo, B.S.**[1,2], **Randall Lee, M.D., Ph.D.**[1,4], **David Schultz, Ph.D.**[5], **Jeffrey Lotz, Ph.D.**[6], and **Song Li, Ph.D.**[1,2,*]

[1]UCSF and UC Berkeley Joint Graduate Group in Bioengineering, University of California, Berkeley, CA 94720

[2]Department of Bioengineering, University of California, Berkeley, CA 94720

[3]Department of Neurological Surgery, University of California, San Francisco, CA 94143

[4]Department of Medicine and CVRI, University of California, San Francisco, CA 94143

[5]Department of Mechanical Engineering, University of California, Berkeley, CA 94720

[6]Department of Orthopaedic Surgery, University of California, San Francisco, CA 94143

Abstract

Objective—We developed small diameter vascular grafts with a microstructure similar to native matrix fibers and with chemically modified microfibers to prevent thrombosis.

Methods and Results—Microfibrous vascular grafts (1-mm internal diameter) were fabricated by electrospinning and hirudin was conjugated to the poly (*l*-lactic acid) (PLLA) microfibers through an intermediate linker of poly(ethylene glycol) (PEG). The modified microfibrous vascular grafts were able to reduce platelet adhesion/aggregation onto microfibrous scaffolds, and immobilized hirudin suppressed thrombin that may interact with the scaffolds. This two-pronged approach to modify microfibrous vascular graft showed significantly improved patency (from 50% to 83%) and facilitated endothelialization, and the microfibrous structure of the vascular grafts allowed efficient graft remodeling and integration, with the improvement of mechanical property (elastic modulus) from 3.5 MPa to 11.1 MPa after 6 months of implantation.

Conclusions—Microfibrous vascular grafts with anti-thrombogenic microfibers can be used as small-diameter grafts with excellent patency and remodeling capability.

Keywords

Vascular graft; small diameter; microfibers; biomaterials; hirudin

[*]To whom correspondence should be addressed: Song Li, Ph.D., Department of Bioengineering, University of California, B108A Stanley Hall, Berkeley, CA 94720-1762. song_li@berkeley.edu. Fax: (510) 666-3381, Phone: (510) 666-2799.

DISCLOSURE
None

INTRODUCTION

Arterial replacement is a common treatment for vascular diseases, with over 500,000 vascular grafts being used in the bypass procedures of coronary and peripheral arteries each year. However, small-diameter synthetic vascular grafts frequently have issues with thrombosis and occlusion. Several methods have been developed to construct tissue-engineered cellular vessels by using vascular cells [1–4]. Recently, we and others have shown that bone marrow cells can be used to construct vascular grafts [5–7], and bone marrow mesenchymal stem cells (MSCs) can resist platelet adhesion and are anti-thrombogenic *in vivo* when seeded onto electrospun fibrous scaffolds [5]. Since a cellular graft takes days to weeks to construct and special care needs to be taken during preservation, shipping and surgery, in this project, we take an alternative approach by fabricating chemically modified acellular microfibrous vascular grafts that can be made available off-the-shelf.

In the past two decades, both decellularized native matrix and synthetic materials have been used to engineer vascular grafts [8–11]. Synthetic biodegradable polymers such as poly(lactic acid), poly(glycolic acid) and their co-polymers have also been used to make porous vascular grafts by using techniques such as solvent casting and particulate-leaching [3, 12–14]. In native blood vessels, collagen and elastin fibers are the major matrix components that provide the structural and mechanical support. To simulate the micro and nano structure of native extracellular matrix (ECM), we and others have used electrospinning technique [15, 16] to fabricate fibrous scaffolds for vascular graft construction [5, 17–22]. To maintain the patency of vascular grafts, cell seeding or surface modification is needed to generate a non-thrombogenic luminal surface. Although it has been shown that seeding vascular cells and bone marrow cells into the grafts can improve the patency of vascular grafts, whether chemical modification of microfibers can generate non-thrombogenic grafts has not been addressed. Here we engineered the chemical property of microfibers to fabricate acellular vascular grafts that are non-thrombogenic and have long-term patency.

Hirudin is a polypeptide of 65 to 66 amino acids derived from the saliva of the medicinal leech *Hirudo medicinalis*. It is the most potent, naturally occurring specific inhibitor of thrombin. In this study, we conjugated hirudin to the poly (*l*-lactic acid) (PLLA) microfibers through an intermediate linker of poly(ethylene glycol) (PEG). The PEG layer was able to reduce platelet adhesion/aggregation onto microfibrous scaffolds, and immobilized hirudin could suppress thrombin that may interact with the scaffolds. This two-pronged approach to modify the microfibrous vascular grafts showed improved patency and facilitated endothelialization, and the microfibrous structure allowed efficient graft remodeling and integration.

METHODS

Microfibrous Scaffold Fabrication and Characterization

A 20% weight/volume solution of PLLA (Lactel Absorbable Polymers, Pelham, AL, 1.09 dL/g inherent viscosity) was formulated using 1,1,1,3,3-hexafluoro-2-propanol (HFIP). The mixture was sonicated for 30 minutes or until all of the PLLA crystals were completely dissolved. Electrospinning was performed [5, 23, 24] with modifications by using a novel setup with a rotating stainless steel mandrel (1-mm diameter; 75 revolutions per minute) and a spinneret that automatically moved back and forth in the longitudinal direction of a mandrel to achieve a uniform thickness of the conduit longitudinally. The negative voltage of 4.5 kilovolts (kV) was applied to the mandrel and a positive voltage of 4 kV was applied to the spinneret by using a high voltage generator (Gamma High Voltage, Ormond Beach, FL). The electrospinning process was allowed to proceed until an approximately 200-μm wall thickness was achieved. The conduit was removed from the mandrel and placed into a vacuum desiccator for 24 hours to evaporate any residual HFIP. The quality, thickness and porosity of the

microfibers were inspected using a Hitachi S-5000 scanning electron microscope. The conduit was trimmed into 7-mm length segments, sterilized in 70% isopropanol, placed under germicidal ultra-violet light for 30 minutes, and washed three times with phosphate buffer saline (PBS).

Hirudin-PEG Conjugation

Di-amino polyethylene glycol (Di-NH2-PEG ; MW 3350; Sigma Aldrich) was covalently linked through the carboxyl groups on the PLLA microfibers of the grafts by using the zero-length cross linkers 1-ethyl-3-(3-dimethylaminopropyl)carbodiimide hydrochloride (EDC) and N-hydroxysulfosuccinimide (Sulfo-NHS) (Pierce Biotechnology, Rockford, IL) [23]. The C-terminus of hirudin (Sigma) was covalently attached to the amine groups on the di-NH2-PEG molecules via EDC and Sulfo-NHS. Afterwards the conduits were incubated with a solution of 100 mg/mL glycine in PBS for 30 minutes at room temperature to wash away and block any remaining amine reactive sites created by crosslinking reagents EDC and Sulfo-NHS. The conduits were washed with PBS three times. To verify that hirudin was linked to nanofibers, immobilized hirudin was stained by using a rabbit antibody against hirudin (American Diagnostica, Inc, Stamford, CT) and a FITC-conjugated goat anti-rabbit antibody (Jackson ImmunoResearch Inc, West Grove, PA).

Platelet Adhesion onto Microfibrous Scaffolds

Platelet-rich plasma from healthy human volunteers was collected [5] and incubated for 30 min on the microfibrous scaffolds with or without conjugation: PLLA, PEG-PLLA and hirudin-PEG-PLLA. Samples were processed and analyzed using two techniques: scanning electron microscopy (SEM) and immunofluorescence staining with 1:100 mouse anti-human CD41 antibody (Lab Vision, Fremont, CA). The total number of adherent platelets from these four images was summed, and the results from multiple experiments from three individual donors were subjected to analysis of variance (ANOVA). A Holm's t-test was used to calculate statistical significance for $P<0.05$.

Animal Studies

All procedures were approved by the Institutional Review Board Service and Institutional Animal Care and Use Committee at the University of California, San Francisco. Female Sprague Dawley rats (200 – 240 grams) were obtained from the Charles River animal facility. The rats were anesthetized with 2.0% isoflurane in 70% nitrous oxide and 30% oxygen. The right common carotid artery was dissected, clamped and transected and the graft was sutured end-to-end with 10-0 interrupted stitches. No heparin or any other anti-coagulant was used at any point prior to, during or after the implantation procedure. For 1-month studies, 12 animals were used in each experimental group. For 6-month studies, 8 animals were used in each experimental group. After 1 to 6 months, the animals were re-anesthetized, the vascular grafts were resected and washed with heparinized saline to remove remaining blood.

Histological Analysis

For histological analysis, the sample was placed into OCT (Sigma Aldrich) and cryo-preserved at −20°C. Cryosections were taken at 10-μm thicknesses. Immunohistochemical staining was used to analyze the tissue sections with the following primary antibodies: CD31 (BD Biosciences, San Jose, CA), myosin heavy chain (Santa Cruz Biotechnology) and CD68 (Santa Cruz Biotechnology). Immunohistochemistry images were captured with a Zeiss Axioskop 2 MOT microscope.

En Face Immunofluorescence Staining for Endothelial Cells (ECs)

Freshly explanted grafts were transected longitudinally and fixed with 4% paraformaldehyde for 15 minutes. The samples were washed with PBS, blocked with 1% BSA and incubated with mouse anti-rat CD31 antibody and Alexa-Fluor 488 secondary antibody The samples were washed and mounted onto a slide such that the luminal surface of the graft was in contact with the coverslip.

Mechanical Testing

Freshly explanted vascular grafts were cut into 3-mm wide ring segments. The tensile strength in the circumferential direction of these rings was tested by using a custom-built soft tissue tester. Two 0.016-inch diameter stainless steel rods were placed through the lumen of the ring segment of the graft, and attached to polycarbonate compression grips. The sample was then loaded onto the mechanical tester, and the applied force and deformation were recorded every second via Labview v4.0 software (National Instruments, Austin, TX). To obtain stress, the cross sectional area of the sample was measured by histological analysis of adjacent cross sections and calculated by using the following formula: 2*(width of the ring)*(wall thickness).The elastic modulus was calculated based on the applied force, graft deformation and the dimensions (thickness and width) of the rings [25].

RESULTS

Direct fabrication of microfibrous tubular graft with a micro structure similar to native matrix fiber

By directly electrospinning polymer fibers onto a rotating mandrel, we successfully made microfibrous tubular grafts (Figure 1A). This is a significant progress towards making seamless microfibrous grafts. The PLLA microfibers made by electrospinning formed a structure (Figure 1B) similar to native matrix fibers. The average diameter of the fibers was approximately 2 microns. As seen in the image, electrospinning process resulted in a highly porous and random structure of fibers, which is excellent tissue engineering scaffold.

Microfibers could be modified by using PEG and hirudin

PEG is capable of creating a brush-like layer onto various surfaces and was used to create a protein and platelet repulsive surface on the PLLA microfiber scaffold. We first conjugated PEG onto microfibers, and then linked hirudin to the end of PEG molecule (Figure 1C). The purpose was to use PEG to resist protein adsorption and platelet adhesion and use hirudin to inactivate thrombin that reached the luminal surface of the vascular grafts. The successful conjugation of PEG and hirudin onto microfibers was confirmed by immunostaining for hirudin, which showed the coating of hirudin on individual microfibers (Figure 1D).

PEG and hirudin-PEG conjugated surfaces reduced the number and aggravation of adherent platelets

To determine whether the grafts modified by PEG and hirudin-PEG can reduce platelet adhesion, platelets were incubated with un-treated grafts and PEG- or hirudin-PEG-modified grafts. As shown in Figure 2A–F, both CD41 staining for platelets and SEM showed that microfibrous scaffolds with conjugated PEG and hirudin-PEG had fewer numbers of platelets on their surfaces than untreated microfibrous scaffolds. The reduction of platelet adhesion on PEG and hirudin-PEG microfibrous scaffolds was statistically significant (Figure 2E), which may help reduce the possibility of early *in vivo* graft failures due to thrombosis and platelet adhesion/activation. The similar reduction of platelet adhesion by PEG and hirudin-PEG suggested that PEG contributed to this anti-platelet adhesion property.

In addition, SEM demonstrated the morphological characteristics of the platelets on the microfibrous PLLA scaffolds. The adherent platelets on the untreated surfaces appeared to have “spiky” protrusions and pseudopods, indicating that they were activated and aggravated by coming into contact with the microfiber sample (Figure 2D). In contrast, fewer adherent platelets were found on the surfaces modified by PEG or hirudin-PEG, and these platelets did not have the same “spiky” protrusions as on the control samples (Figure 2E–F).

PEG and hirudin-PEG modified grafts improved patency rates *in vivo*

To compare the anti-thrombogenic property of the vascular grafts in vivo, untreated microfibrous grafts and the grafts modified with PEG or hirudin-PEG were implanted into the common carotid artery of rats for 1 month. Patency was determined by ultrasound and necropsy. Graft patency was determined by the unobstructed flow of blood through the graft. At 1 month, 6 out of 12 (50%) untreated grafts were patent, 9 out of 12 (75%) PEG grafts were patent, and 10 of 12 (83%) hirudin-PEG grafts were patent. These results suggest that both PEG and hirudin improved the patency rate.

To further determine the long-term remodeling of the patent grafts, hirudin-PEG-modified grafts were implanted for 6 months. At 6 months, 6 of the 7 (86%) implanted hirudin-PEG grafts were patent. Based on histological analysis, the failed grafts were clogged with thrombus, indicating the imperfect patency rate was related to easiness of clotting in 1-mm grafts.

The patent grafts from hirudin-PEG group are shown in Figure 3 as representatives. Figure 3A shows a stereomicrograph image of an implanted graft moments after the anastomosis was completed. The porous structure of the graft was immediately filled with red blood cells and other cellular components, and the color of the graft changed from milky white to a red. The interrupted suture technique did not result in any of bleeding or leakage at the anastomotic sites. Good blood flow was observed at both the proximal and distal ends of the graft.

After 1 month, there was visible angiogenesis in the wall of the graft (Figure 3B). The presence of newly formed micro-vessels indicates the integration of the graft into the host’s vasculature. In addition, it suggests that the graft is becoming a living part of the host and that angiogenesis is necessary to supply nutrients, oxygen and other diffusible chemicals to the local cells that reside within and around the graft. It was observed that the amount of angiogenesis was slightly less in the 6-month grafts (Figure 3C), suggesting that the angiogenesis was part of an acute wound healing process in the graft.

A suture site, as well as the characteristics of the graft after 1 month was captured by a stereomicroscope (Figure 3D). The luminal surface was presented by transecting the graft along the longitudinal direction. The anastomotic sites were free of thrombosis and intimal hyperplasia.

Graft patency was also monitored by using Doppler Duplex (Figure 3E) and magnetic resonance imaging (MRI) (Figure 3F), showing normal flow rate in the patent grafts.

Endothelialization, cellular infiltration and organization

The patent grafts (either in the untreated group or hirudin-treated group) showed similar histological results. Therefore, only hirudin-treated grafts are shown as representatives. Patent grafts (exemplified by hirudin-PEG grafts in Figure 4) showed very little signs of thrombosis and/or intimal hyperplasia on the luminal walls of the graft at either the 1 (Figure 4A) or 6-month (Figure 4B) time point. It is evident that the neo- tissue formation on the outer surface of the grafts was significant at both time points. The neo- tissue in the 1-month samples had a highly porous and loose tissue structure on the outside of the graft (Figure 4C). On the other hand, the 6-month sample had dense neo-tissue with extracellular matrix alignment in the

circumferential direction (Figure 4D). The nucleus staining revealed that there were cells within the walls of the graft and the neo-tissue in the outer layer (Figure 4E–F), suggesting that the graft is capable of supporting cellular ingrowth.

Endothelialization on the luminal surface is important to maintain the long-term patency of vascular grafts. All patent samples had complete endothelial coverage at the 1 (Figure 5 A–C) and 6-month (Figure 5D) time points. The newly formed capillaries and micro-vessels were evident in the neo-tissue of the graft (Figure A, C, D), which suggests the remodeling of the grafts. Immunofluorescent *en face* staining revealed that ECs had aligned in the flow direction and had morphological appearance similar to ECs in native arteries (Figure 5B).

Smooth muscle cell (SMC) presence and organization are also important for the long-term stability of vascular grafts. Interestingly, SMC staining showed that SMCs were mostly in the neo-tissue surrounding the grafts after 1 month (Figure 5E) and 6 months (Figure 5F) post-implantation. The 6-month sample (Figure 4F) had a clearly defined band of SMCs that are highly organized and aligned in the circumferential direction. There was no sign of a neo-intima or intimal hyperplasia in these patent grafts.

The inflammatory responses to the PLLA vascular graft was monitored via immunostaining of CD68, a cell surface marker for monocytes and macrophages (Figure 5G–H). There were few CD68 positive cells within the walls of the graft, suggesting minimal inflammatory responses to the grafts.

Mechanical strength increased after *in vivo* remodeling

Mechanical strength is critical for the long-term stability of the grafts. We performed mechanical tests by using rings of the non-implanted grafts and explanted grafts (Figure 6A). Representative stress-strain curve of explanted grafts at 1- and 6-month time points are shown in Figure 6B. The elastic modulus of the grafts before implantation was about 3.5 MPa (Figure 6C). After 1 month, a slight increase of elastic modulus (5.5 MPa) of the grafts was observed. After 6 months of implantation, the grafts had a significant increase of elastic modulus (11.1 MPa), suggesting a significant remodeling of the grafts *in vivo*.

DISCUSSION

In this study, we developed small diameter vascular grafts with high patency rates by using chemical modification of microfibers. These modified acellular grafts showed higher patency rates, great remodeling and little intimal thickening for 1 and 6 months. To fabricate tubular nanofibrous scaffolds, we have developed an electrospinning system with a rotating mandrel. The rotating mandrel served as the collector of the electrospun nanofibers, and the internal diameter of the tubular scaffolds is the same as the diameter of the mandrel. In this study, the internal diameter of the grafts was 1 mm, and it is feasible to make tubular grafts with much smaller diameter. Compared to previous fabrication methods such as solvent casting and particulate-leaching, the microfibrous structure of electrospun tubular scaffolds provides a matrix more similar to that in native ECM of blood vessels.

In vitro assessment of the scaffold revealed several interesting points that eventually led to the enhanced *in vivo* vascular patency in both the acute and chronic vascular grafts. We showed the ability of the PEGylated surface to repel and maintain the quiescent state of the platelets. The platelets and presumably other serum proteins were unable to attach onto the brush-like layer of the PEG. Both platelet adhesion and aggravation were reduced on PEG surface, indicating the biological effects of chemical modification. Hirudin-PEG did not decrease platelet adhesion further compared to PEG surface, suggesting that the resistance to platelet adhesion could be attributed to PEG layer. Consistently, *in vivo* studies showed that the grafts

modified with PEG and hirudin-PEG significantly improved the patency rate of the grafts. The slightly higher patency rate of hirudin-PEG grafts (10 out of 12) suggests that hirudin may have additional beneficial effect, e.g, inhibition of thrombin activity.

Endothelialization and sufficient mechanical strength are two critical aspects to maintain the long-term stability of vascular grafts. The chemically modified grafts were able to prevent early thrombosis and allow ECs to form monolayer so that long-term patency was achieved. Both histological staining and *en face* staining showed excellent endothelialization in our grafts at 1 and 6 month time points, which contributed to the long-term patency. The significant increase of the mechanical strength of the grafts at 6 months suggests that there was an increase of matrix synthesis in and surrounding the grafts *in vivo*. Based on histological analysis, it is likely that the neo-tissue on the outer surface of the grafts contributed significantly to the enhanced mechanical strength. The values of elastic modulus for the grafts are similar to those of native arteries in rats (tens of MPa).

The microfibrous grafts were integrated very well into native vasculature, supported by the evidence of angiogenesis and SMC recruitment in the outer layer of the graft. The minimal inflammatory response suggests that the PLLA microfibers are biocompatible materials for vascular regeneration. It is possible that cells could migrate into the grafts from both inside and outside surfaces[8]. For example, ECs on the luminal surface could be from microvessels outside the graft, the arteries at two ends of the graft and circulating cells (e.g., endothelial progenitor cells) in the blood stream. Additional work needs to be performed to investigate the origin of ECs. The organization of the SMCs in the neo-tissue outside of the graft is an interesting observation. These SMCs could be from the arteries connected to the grafts or from the surrounding tissues. This is in contrast to the previous observation of SMCs underneath of endothelium in MSC-seeded nanofibrous grafts [5]. It is likely that cell-seeded grafts allow better cell recruitment and infiltration into the grafts. Alternatively, since those cell-seeded grafts had fiber alignment in the circumferential direction, the alignment of fibers in the cellular grafts could facilitate cell infiltration into the three-dimensional structure of the scaffold. These possibilities need to be examined in future studies, and the electrospun scaffolds could be engineered to further increase cell infiltration.

In the case of other synthetic materials, there were reports on the use of hirudin to modify Dacron and ePTFE grafts. For example, previous study showed the successful conjugation of hirudin onto Dacron surface but *in vivo* performance was not reported [26]. Interestingly, direct coating of ePTFE grafts with hirudin also resulted in excellent patency in larger grafts (4 mm in diameter) [27]. A potential disadvantage of non-covalent coating is the lack of control of surface binding efficiency and hirudin retention on the surface. It will be useful to compare the retention of hirudin on the luminal surface of the grafts with and without conjugation under hemodynamic condition.

The use of bioabsorbable microfibrous scaffolds for vascular grafts make it possible to regenerate native blood vessels. The slow degradation rate of biopolymers such as PLLA maintains the mechanical strength of the grafts long enough and allows gradual replacement of synthetic scaffolds by native matrix with time. The microfibrous structure provides a mechanically stable module until cellular infiltration and scaffold remodeling eventually lead to a tissue-like product capable of self-support. In this study with 6-month implantation, no significant degradation of the grafts was observed because the half-degradation time of PLLA is more than a year.

The methods to directly fabricate tubular constructs by using electrospinning make it possible to scale up the production of more uniform and better quality grafts, opposed to the rolling technique previously used. The *in vitro* and *in vivo* analysis of the functional performance of

the microfibrous vascular grafts provides insight into the mechanisms of the remodeling and regeneration of a blood vessel with microstructure. The ability to now create anti-thrombogenic small diameter vascular grafts makes it more feasible to offer vascular grafts available off-the-shelf.

Acknowledgments

The authors would like to thank Benjamin Lee and Henry Liu for their help with graft preparation and histology and Michael Wendland for his help with magnetic resonance imaging.

SOURCES OF FUNDING

This work was supported in part by NIH Grants HL 078534 (to S.L.), HL 083900 (to S.L.), the California Institute for Regenerative Medicine Training Grant T1-0007 (to C.K.H.) and NIGMS-IMSD Training Grant GM56847 (to R.R.R.J.).

REFERENCES

1. Weinberg CB, Bell E. A blood vessel model constructed from collagen and cultured vascular cells. Science 1986;231:397–400. [PubMed: 2934816]
2. L'Heureux N, Dusserre N, Konig G, Victor B, Keire P, Wight TN, Chronos NA, Kyles AE, Gregory CR, Hoyt G, Robbins RC, McAllister TN. Human tissue-engineered blood vessels for adult arterial revascularization. Nat Med 2006;12:361–365. [PubMed: 16491087]
3. Niklason LE, Gao J, Abbott WM, Hirschi KK, Houser S, Marini R, Langer R. Functional arteries grown in vitro. Science 1999;284:489–493. [PubMed: 10205057]
4. Nerem RM, Seliktar D. Vascular tissue engineering. Annu Rev Biomed Eng 2001;3:225–243. [PubMed: 11447063]
5. Hashi CK, Zhu Y, Yang GY, Young WL, Hsiao BS, Wang K, Chu B, Li S. Antithrombogenic property of bone marrow mesenchymal stem cells in nanofibrous vascular grafts. Proc Natl Acad Sci U S A 2007;104:11915–11920. [PubMed: 17615237]
6. Brennan MP, Dardik A, Hibino N, Roh JD, Nelson GN, Papademitris X, Shinoka T, Breuer CK. Tissue-engineered vascular grafts demonstrate evidence of growth and development when implanted in a juvenile animal model. Ann Surg 2008;248:370–377. [PubMed: 18791357]
7. Gong Z, Niklason LE. Small-diameter human vessel wall engineered from bone marrow-derived mesenchymal stem cells (hMSCs). Faseb J 2008;22:1635–1648. [PubMed: 18199698]
8. Clowes AW, Kirkman TR, Reidy MA. Mechanisms of arterial graft healing. Rapid transmural capillary ingrowth provides a source of intimal endothelium and smooth muscle in porous PTFE prostheses. Am J Pathol 1986;123:220–230. [PubMed: 3706490]
9. Huynh T, Abraham G, Murray J, Brockbank K, Hagen PO, Sullivan S. Remodeling of an acellular collagen graft into a physiologically responsive neovessel. Nat Biotechnol 1999;17:1083–1086. [PubMed: 10545913]
10. Isenberg BC, Williams C, Tranquillo RT. Small-diameter artificial arteries engineered in vitro. Circ Res 2006;98:25–35. [PubMed: 16397155]
11. Jordan SW, Haller CA, Sallach RE, Apkarian RP, Hanson SR, Chaikof EL. The effect of a recombinant elastin-mimetic coating of an ePTFE prosthesis on acute thrombogenicity in a baboon arteriovenous shunt. Biomaterials 2007;28:1191–1197. [PubMed: 17087991]
12. van der Lei B, Wildevuur CR, Dijk F, Blaauw EH, Molenaar I, Nieuwenhuis P. Sequential studies of arterial wall regeneration in microporous, compliant, biodegradable small-caliber vascular grafts in rats. J Thorac Cardiovasc Surg 1987;93:695–707. [PubMed: 3573782]
13. Mooney DJ, Mazzoni CL, Breuer C, McNamara K, Hern D, Vacanti JP, Langer R. Stabilized polyglycolic acid fibre-based tubes for tissue engineering. Biomaterials 1996;17:115–124. [PubMed: 8624388]
14. Wake MC, Gupta PK, Mikos AG. Fabrication of pliable biodegradable polymer foams to engineer soft tissues. Cell Transplant 1996;5:465–473. [PubMed: 8800514]

15. Chew SY, Wen Y, Dzenis Y, Leong KW. The role of electrospinning in the emerging field of nanomedicine. Curr Pharm Des 2006;12:4751–4770. [PubMed: 17168776]

16. Liang D, Hsiao BS, Chu B. Functional electrospun nanofibrous scaffolds for biomedical applications. Adv Drug Deliv Rev 2007;59:1392–1412. [PubMed: 17884240]

17. Boland ED, Matthews JA, Pawlowski KJ, Simpson DG, Wnek GE, Bowlin GL. Electrospinning collagen and elastin: preliminary vascular tissue engineering. Front Biosci 2004;9:1422–1432. [PubMed: 14977557]

18. He W, Yong T, Teo WE, Ma Z, Ramakrishna S. Fabrication and endothelialization of collagen-blended biodegradable polymer nanofibers: potential vascular graft for blood vessel tissue engineering. Tissue Eng 2005;11:1574–1588. [PubMed: 16259611]

19. Stitzel J, Liu J, Lee SJ, Komura M, Berry J, Soker S, Lim G, Van Dyke M, Czerw R, Yoo JJ, Atala A. Controlled fabrication of a biological vascular substitute. Biomaterials 2006;27:1088–1094. [PubMed: 16131465]

20. El-Kurdi MS, Hong Y, Stankus JJ, Soletti L, Wagner WR, Vorp DA. Transient elastic support for vein grafts using a constricting microfibrillar polymer wrap. Biomaterials 2008;29:3213–3220. [PubMed: 18455787]

21. Soffer L, Wang X, Zhang X, Kluge J, Dorfmann L, Kaplan DL, Leisk G. Silk-based electrospun tubular scaffolds for tissue-engineered vascular grafts. J Biomater Sci Polym Ed 2008;19:653–664. [PubMed: 18419943]

22. Nieponice A, Soletti L, Guan J, Deasy BM, Huard J, Wagner WR, Vorp DA. Development of a tissue-engineered vascular graft combining a biodegradable scaffold, muscle-derived stem cells and a rotational vacuum seeding technique. Biomaterials 2008;29:825–833. [PubMed: 18035412]

23. Patel S, Kurpinski K, Quigley R, Gao H, Hsiao BS, Poo MM, Li S. Bioactive nanofibers: synergistic effects of nanotopography and chemical signaling on cell guidance. Nano Lett 2007;7:2122–2128. [PubMed: 17567179]

24. Huang NF, Patel S, Thakar RG, Wu J, Hsiao BS, Chu B, Lee RJ, Li S. Myotube assembly on nanofibrous and micropatterned polymers. Nano Lett 2006;6:537–542. [PubMed: 16522058]

25. Wagner DR, Lotz JC. Theoretical model and experimental results for the nonlinear elastic behavior of human annulus fibrosus. J Orthop Res 2004;22:901–909. [PubMed: 15183453]

26. Phaneuf MD, Berceli SA, Bide MJ, Quist WC, LoGerfo FW. Covalent linkage of recombinant hirudin to poly(ethylene terephthalate) (Dacron): creation of a novel antithrombin surface. Biomaterials 1997;18:755–765. [PubMed: 9158859]

27. Heise M, Schmidmaier G, Husmann I, Heidenhain C, Schmidt J, Neuhaus P, Settmacher U. PEG-hirudin/iloprost coating of small diameter ePTFE grafts effectively prevents pseudointima and intimal hyperplasia development. Eur J Vasc Endovasc Surg 2006;32:418–424. [PubMed: 16682237]

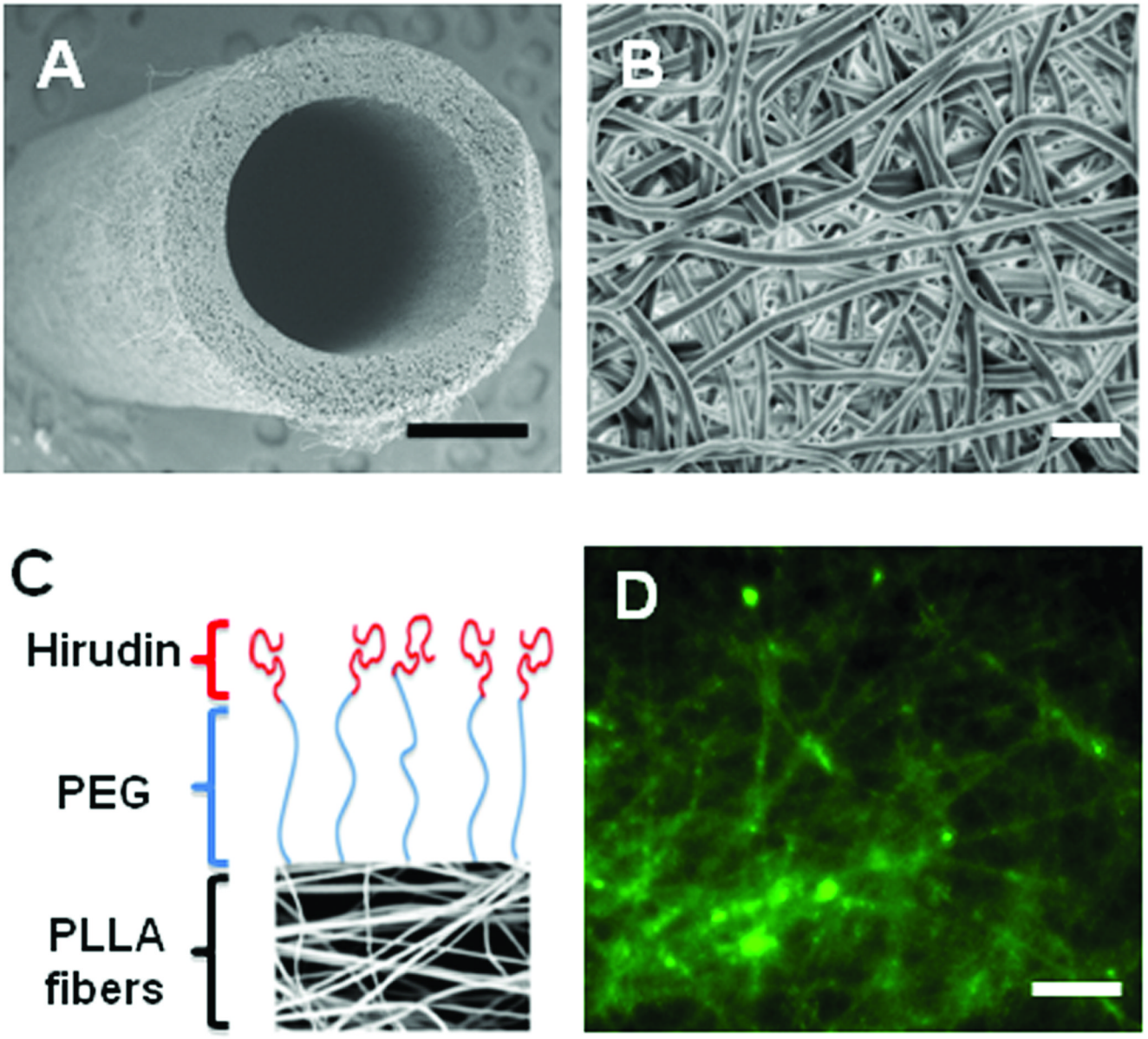

Figure 1.
Structure and chemical modification of microfibrous vascular grafts. (A) SEM image of the electrospun, microfibrous vascular graft. Scale bar = 0.5 mm. (B) SEM of the luminal surface of the electrospun vascular graft. Scale bar = 10 μm. (C) Conjugation of PEG and hirudin to PLLA. (D) Immunostaining of hirudin on nanofibers. Scale bar = 20 μm.

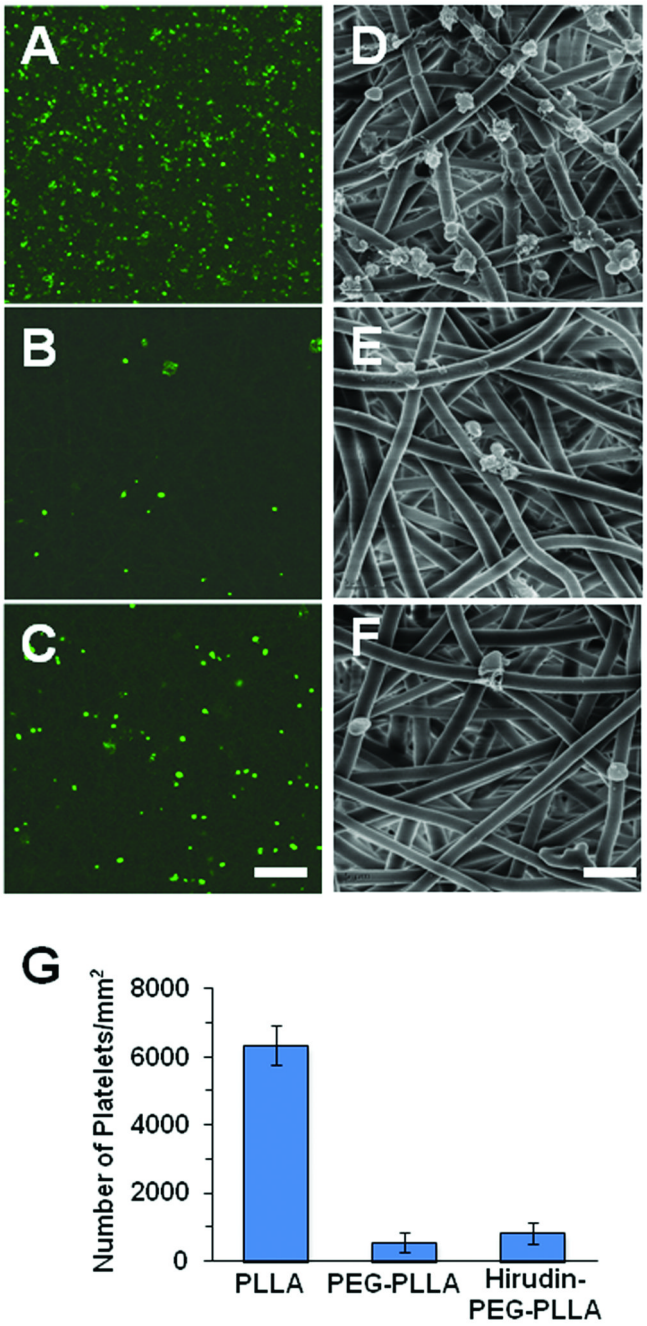

Figure 2.

Representative images of human platelets seeded onto PLLA (A, D), PEG-PLLA (B, E) and hirudin-PEG-PLLA (C, F) surfaces. CD41 mouse anti-human antibody and Alexa Fluor 488 secondary were used to stain platelets on PLLA (A), PEG-PLLA (B) and hirudin-PEG-PLLA (C) surfaces. SEM revealed the morphology and adhesion of platelet on PLLA (D), PEG-PLLA (E) and hirudin-PEG-PLLA (F) surfaces. Scale Bar = 50 μm in A–C, scale Bar = 5 μm D–F. (G) The number of platelets bound to each surface. *P<0.05, n=4. Bar graph shows mean ±standard deviation.

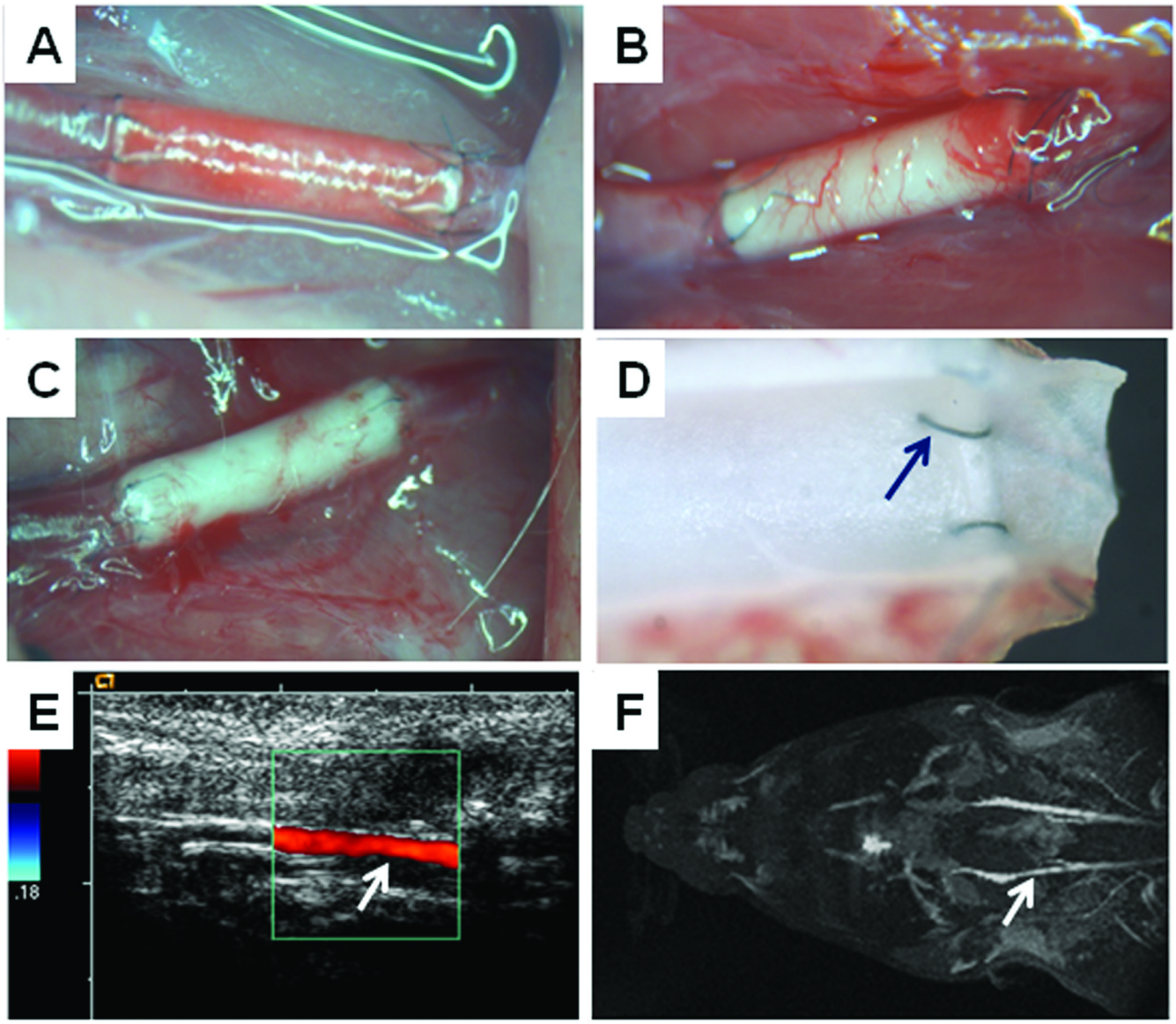

Figure 3.
Images of 1-mm internal diameter hirudin-PEG-PLLA grafts *in vivo*. (A) Image taken immediately after implantation of the graft. (B) After 1 month. (C) After 6 months. (D) Stereomicrograph image of the luminal surface of a freshly explanted 1-month sample. (E) Duplex doppler of the graft taken prior to sacrificing the animal at 6 months. (F) MRI shows symmetric blood flow in the control common carotid artery (top) and the 1-mm internal diameter graft (bottom; indicated by arrow).

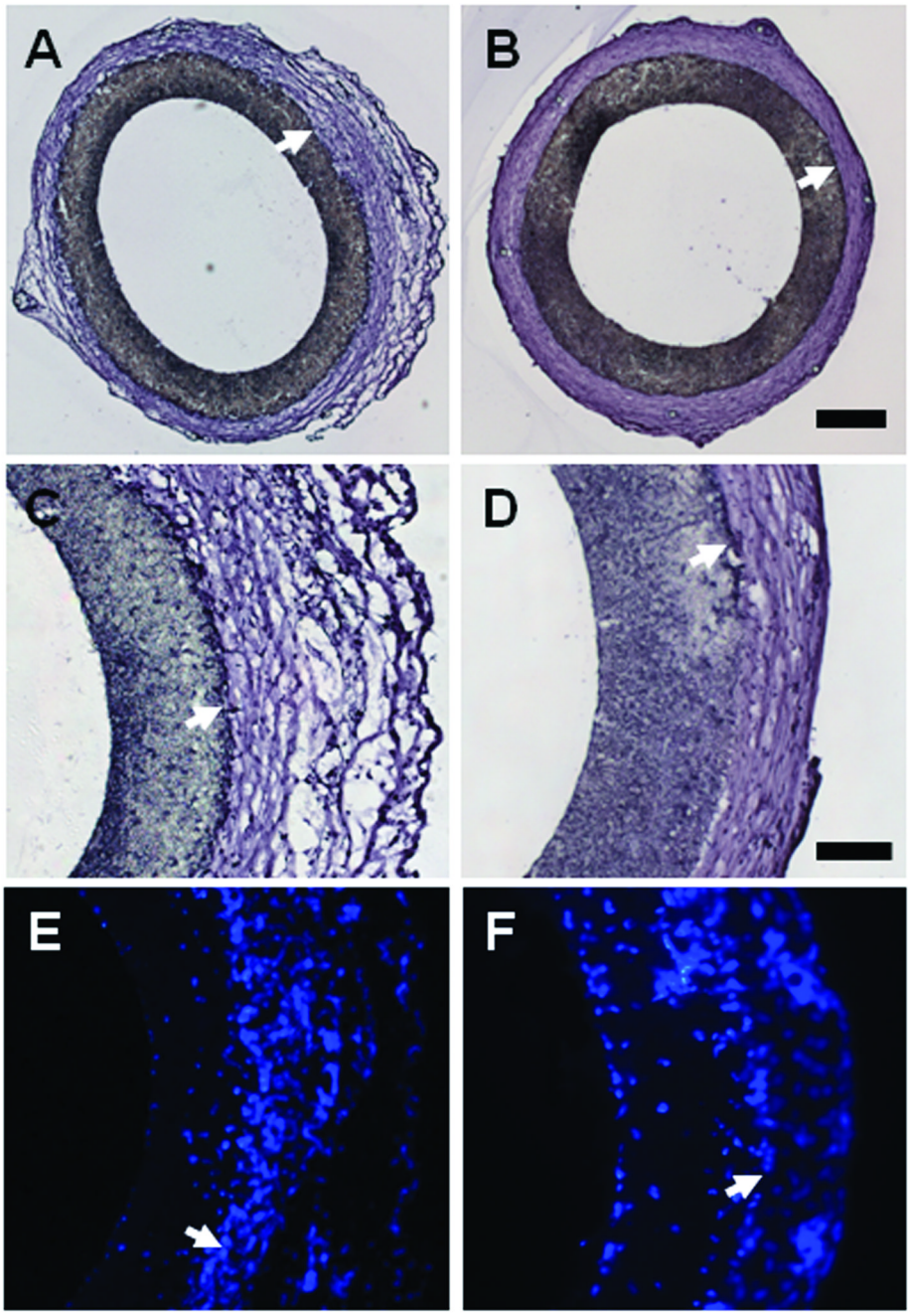

Figure 4.
Cross sections of the explanted hirudin-PEG-PLLA grafts at 1 month (A, C, E) and 6 month (B, D, F) post implantation. Hematoxylin staining (A, B, C, D) showed the patency and structure of the grafts. Nucleus staining by DAPI (E, F) showed the distribution of cells. Arrows 22 indicate the border of the polymer scaffolds. Scale bar in A,B = 250 μm. Scale bar in C, D, E, F = 100 μm.

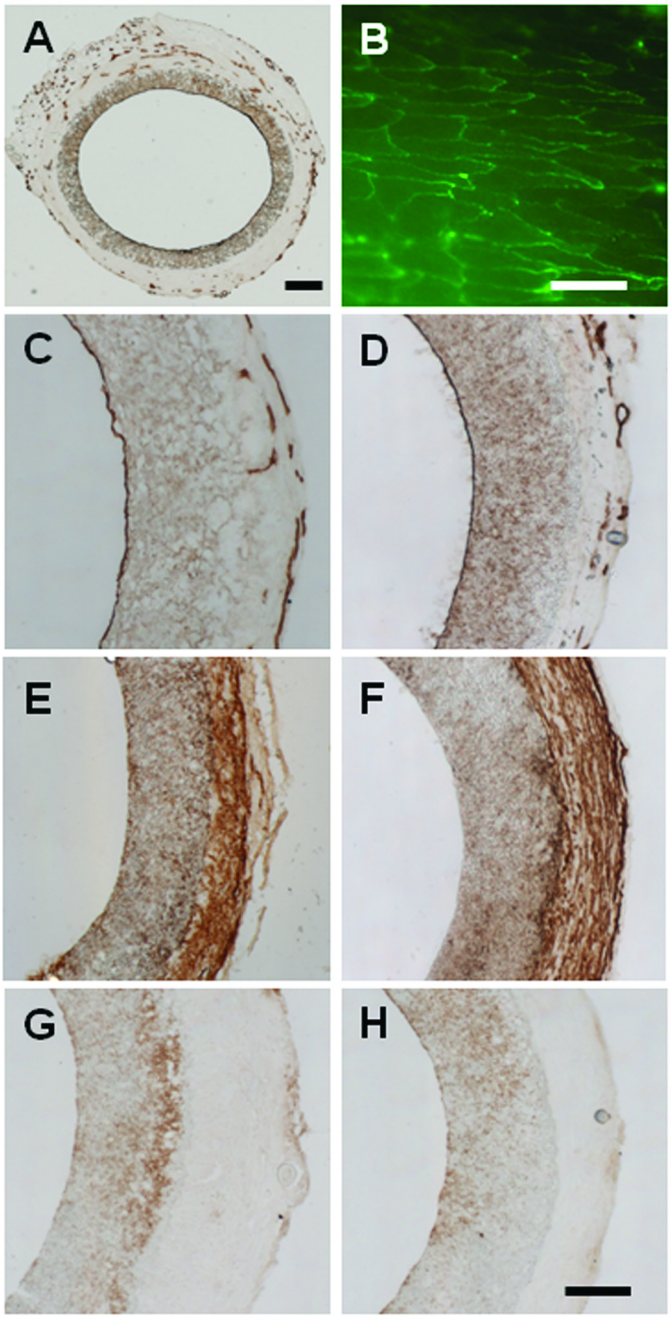

Figure 5.
Endothelialization, SMCs and inflammatory cells in hirudin-PEG-PLLA grafts. ECs were stained by using CD31 antibody (A–D), SMCs were stained by using SM-MHC antibody (E–F), and monocytes and macrophages were stained by using CD68 antibody (G–H). (A and C) Complete endothelial cell coverage and adventitial angiogenesis seen after 1 month post implantation. (B) *En face* staining shows complete endothelialization after 1 month. (D) Complete endothelialization after 6-month implantation. (E) Immunostaining for SM-MHC at 1-month. (F) Immunostaining for SM-MHC at 6 months. (G) CD68 staining at 1 month. (H) CD68 staining after 6-month implantation. Scale bar in A = 200 μm. Scale bar in B = 50 μm. Scale bar for C, D, E, F = 100 μm.

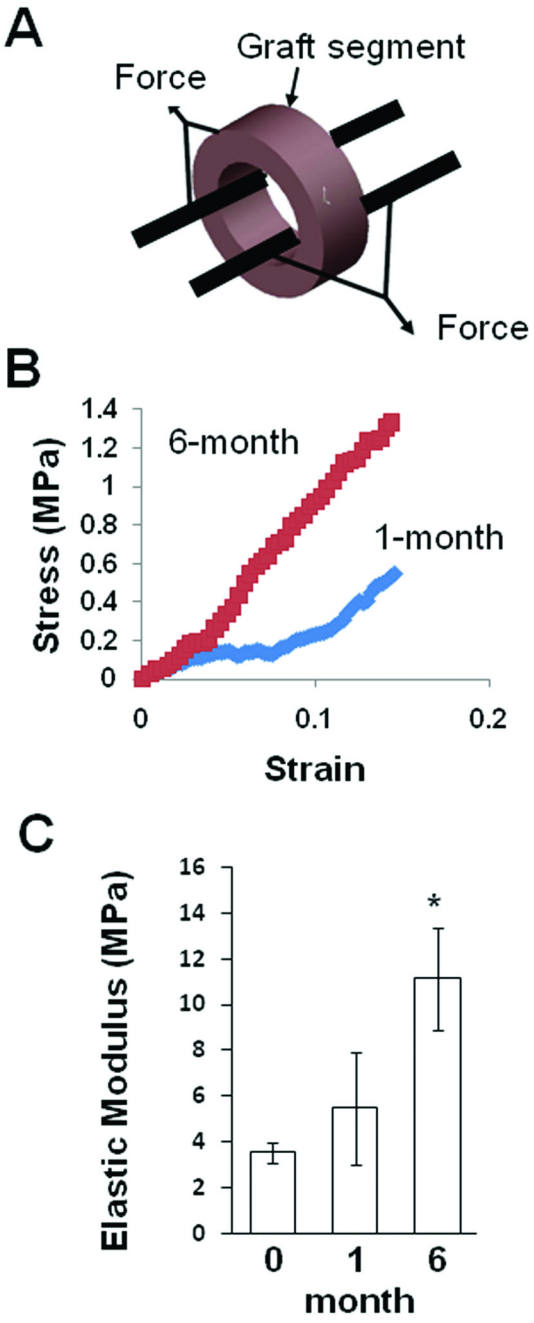

Figure 6.

Mechanical characterization of the tensile strength of hirudin-PEG-PLLA vascular grafts. (A) Two stainless steel rods were placed through the lumen of the ring segment of the graft. The sample was then loaded onto the mechanical tester, and the applied force and deformation were recorded. (B) A typical stress-strain curve of vascular graft at 1- and 6-month implantation. Elastic modulus was calculated from the slope of the curve and graft dimensions. (C) Elastic modulus of grafts without implantation, after 1-month implantation and after 6-month implantation (n=4). * indicates significant difference ($p<0.05$) compared to other groups of samples. Bar graph shows mean±standard deviation.